

Efficient Computation of Display Gamut Volumes in Perceptual Spaces

Carlos Eduardo Rodríguez-Pardo(1), Gaurav Sharma(1), Jon Speigle(2), Xiao-Fan Feng(2), Ibrahim Sezan(2)

(1) ECE Dept. Univ. of Rochester, Rochester, NY 14627-0126

(2) Sharp Laboratories of America, Camas, WA 98607

Abstract

Gamut volume computations in perceptual spaces are useful for optimizing designs of color displays. We develop a useful representation of the gamut of an additive display that facilitates efficient numerical computation of the gamut volume. For three primary systems, our representation coincides with the obvious representation of a three-primary additive gamut, while for multi-primary systems, the representation we develop provides a partition of the device gamut as a disjoint union of displaced three primary gamuts thereby facilitating a computation of the overall gamut volume as the sum of these individual three primary gamut volumes. Based on our representation, we develop and evaluate several alternative numerical schemes for gamut volume computations in perceptual spaces, comparing their accuracy and computational requirements.

1 Introduction

A fundamental choice when designing displays is the selection of the color primaries [1, 2]. In practice, this selection represents a multi-way trade off between the color gamut, dynamic range, power consumption, and material cost and environmental concerns. For optimizing display design, modeling and analysis of display gamuts is therefore of significant interest.

Because most displays are additive devices, their gamut in additive color spaces, such as the CIE XYZ color space [3], can be modeled in a relatively straightforward manner [4–6]. For three primary display systems, computation of the gamut volume in the additive spaces is also straightforward. However, the gamut volume in a linear additive color space correlates very poorly with an observer’s perceptual assessment of the gamut volume. Consequently, for the purposes of display optimization, the gamut volume in a perceptually uniform color space such as CIELAB [3] is much more useful. Unfortunately, it is not feasible to analytically compute the gamut volume in perceptually uniform color spaces and numerical computation is therefore utilized in practice [7].

The difficulty of such numerical computations is compounded by the fact that in perceptual color spaces, display gamuts are usually nonconvex. For multiprimary systems, an additional challenge arises from the fact that for the computation of gamut volume, the gamut representation does not immediately indicate an obvious way for dealing with the degeneracy arising from multiple metameric options available for a given colorimetry.

In this paper, we first develop representations for display gamuts in additive color spaces that facilitate computations of gamut volumes, both in additive and perceptual spaces, particu-

larly focusing on multiprimary display systems where the definition of the display gamut does not naturally lead to such a representation. We then consider different methods for numerical computation of display gamut volume in perceptual color spaces, all based on the gamut representations that we develop for this purpose. We evaluate the accuracy vs computation time trade-offs for the different methods.

The paper is organized as follows. Section 2 presents the mathematical framework for modeling display gamuts in additive color spaces and characterizes the display gamut volume in additive color spaces for both three primary and multi-primary systems. Section 3 considers the computation of gamut volumes, first outlining the computation in additive color spaces and then addressing the computation in perceptual color spaces. Section 4 presents results from tests conducted to evaluate the methods, comparing the accuracy and computation time requirements for the different methods. Section 5 concludes the paper by summarizing the main findings.

2 Display Gamuts for Three Primary and Multiprimary Displays

A color produced by a display system with primaries vectors $\mathbf{p}_1, \mathbf{p}_2, \mathbf{p}_3$, specified in an additive color space, is obtained by a linear combination of the primaries, and can be represented by the tristimulus value

$$t_{\mathbf{p}}(\alpha) = \mathbf{P}\alpha, \quad (1)$$

where $\mathbf{P} = [\mathbf{p}_1, \mathbf{p}_2, \mathbf{p}_3]$ is the *matrix of primaries*, and $\alpha = [\alpha_1, \alpha_2, \alpha_3]^T$ is the vector that determines the relative proportion for the combination of the primaries, whose entries satisfy the constraints $0 \leq \alpha_i \leq 1, i = 1, 2, 3$.

An important characterization for display systems is given in term of the gamut, or the set of colors the device is able to reproduce. Adopting for simplicity the notation of the well known CIE XYZ color space [3]¹, the gamut of the display with matrix of primaries \mathbf{P} , denoted by $\mathcal{G}_{\mathbf{P}}^{XYZ}$, is defined as,

$$\begin{aligned} \mathcal{G}_{\mathbf{P}}^{XYZ} &= \{t_{\mathbf{p}}(\alpha) | \alpha \in [0, 1]^3\} \\ &= \{\mathbf{P}\alpha | \alpha \in [0, 1]^3\} \end{aligned} \quad (2)$$

The maximum luminance combination, usually referred as the *white point*, is obtained when $\alpha_i = 1$, for $i = 1, 2, 3$. Note that

¹Although we use the CIE XYZ space, all definitions and results described here can be applied to other additive color spaces.

from the expression in (2), it is possible to conclude that the definition of gamut corresponds to the definition of the parallelepiped that contain the origin and in the primary vectors as four of its vertexes. In fact, the parallelepiped can be interpreted as the linear transformation represented by the matrix of primaries \mathbf{P} of the unitary cube $[0, 1]^3$, denoted for simplicity by \mathcal{C}^3 , and referred as the *primary space*.

A system with K primaries can be similarly represented by a $3 \times K$ matrix $\mathbf{P} = [\mathbf{p}_1, \mathbf{p}_2, \dots, \mathbf{p}_K]$, where $\mathbf{p}_1, \mathbf{p}_2, \dots, \mathbf{p}_K$ are the coordinates of the primaries in CIEXYZ space. The gamut in CIEXYZ space can then be obtained in a manner exactly analogous to (2) as

$$\mathcal{G}_{\mathbf{P}}^{XYZ} = \left\{ t_{\mathbf{P}}(\alpha) = \mathbf{P}\alpha \mid \alpha \in \mathcal{C}^k \right\}. \quad (3)$$

where the primary space \mathcal{C}^K corresponds to the unitary hypercube of dimension K .

While the mathematical representation of the gamut for a multiprimary system in (3) closely mirrors the representation for the three primary display gamut in (2), unlike the former representation, the latter representation is not particularly well suited for computation of gamut volumes, as we shall subsequently see in Section 3. For this purpose, an alternative and more useful definition is based on the fact that the gamut can be partitioned into parallelepipeds. Specifically, for a system described by a $3 \times K$ matrix of primaries \mathbf{P} we have that,

$$\mathcal{G}_{\mathbf{P}}^{XYZ} = \bigcup_j \mathcal{P}_j, \quad (4)$$

where the summation over j ranges over the $\binom{K}{3}$ possibilities for selecting a set \mathbf{P}_j of three primaries from the K possibilities in \mathbf{P} and $\mathcal{P}_j = \mathcal{G}_{\mathbf{P}_j}^{XYZ} + \beta_j$ is the parallelepiped obtained by displacing the gamut $\mathcal{G}_{\mathbf{P}_j}^{XYZ}$, of the three primary system with primaries \mathbf{P}_j , by the displacement vector β_j . The displacement vector β_j can be expressed as a linear combination of the primaries \mathbf{P} where the coefficients in the linear combination are 0 or 1 and the coefficients corresponding to the primaries in \mathbf{P}_j are necessarily zero. For space reasons, we omit a formal proof of this result and the algorithm for obtaining this representation for a given set of primaries, illustrating the result instead by examples, the first of which we present pictorially. In Fig. 1, the gamuts for a three primary and a multiprimary systems are shown. For the latter case, four parallelepipeds partition the entire gamut, corresponding to $\binom{K}{3}$ possible different choices of the primaries, with $K = 4$. A numerical example illustrating this decomposition is presented in Table 1, for a four primary system from [7] specified by the 4×3 primary matrix

$$\mathbf{P} = [\mathbf{p}_1, \mathbf{p}_2, \mathbf{p}_3, \mathbf{p}_4] \stackrel{\text{def}}{=} \begin{bmatrix} 0.3630 & 0.1539 & 0.0471 & 0.0758 \\ 0.1761 & 0.3700 & 0.3093 & 0.0244 \\ 0.0027 & 0.0179 & 0.1853 & 0.4415 \end{bmatrix}. \quad (5)$$

In Table 1, for each of the four, i.e. $\binom{4}{3}$, parallelepipeds we list the index j , the corresponding matrix of three primaries \mathbf{P}_j , expressed in terms of primaries defined in (5), and the coordinate vector for the shift vector β_j in the space of the primaries \mathbf{P} in (5).

j	\mathbf{P}_j	Coordinates of β_j
1	$[\mathbf{p}_1, \mathbf{p}_2, \mathbf{p}_3]$	$[0, 0, 0, 0]^T$
2	$[\mathbf{p}_1, \mathbf{p}_2, \mathbf{p}_4]$	$[0, 0, 1, 0]^T$
3	$[\mathbf{p}_1, \mathbf{p}_3, \mathbf{p}_4]$	$[0, 0, 0, 0]^T$
4	$[\mathbf{p}_2, \mathbf{p}_3, \mathbf{p}_4]$	$[1, 0, 0, 0]^T$

Table 1. Parallelepiped decomposition for the gamut for the display with primaries in (5).

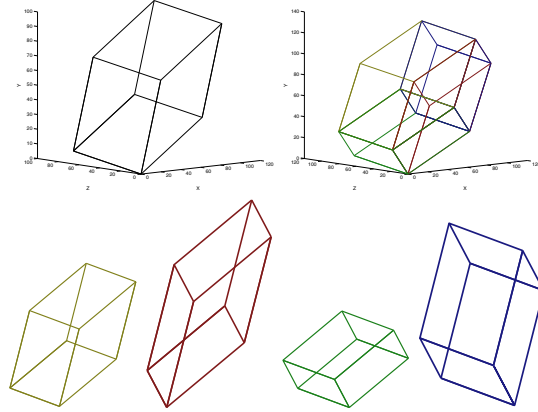


Figure 1. In the top left, the gamut of a system with three primaries that match the chromaticity coordinates for the standard REC-709 and have a white point luminance of 100 (See configuration C_1 in Table 2). In the top right, a multiprimary system obtained by adding a primary with CIEXYZ coordinates $[2.02, 20.02, 20.02]^T$. The gamut for the multiprimary case is composed by the union of disjoint parallelepipeds that are shown in the bottom of the image (not to scale)

3 Display Gamut Volume

3.1 Gamut Volume in Additive Color Spaces

Additive color spaces are three dimensional and are embedded in \mathbb{R}^3 . Therefore, they inherit the results of three dimensional geometry, which can be applied in the manipulation and analysis of display gamuts. For a system with the matrix of primaries \mathbf{P} in CIEXYZ, the gamut volume $V(\mathcal{G}_{\mathbf{P}}^{XYZ})$ is the volume of the parallelepiped enclosed by primaries, and therefore the gamut volume can be defined as [8, pp. 468],

$$V(\mathcal{G}_{\mathbf{P}}^{XYZ}) = |\det(\mathbf{P})|, \quad (6)$$

where, $\det(\cdot)$ and $|\cdot|$ are the determinant the magnitude operators, respectively. Note that $\det(\mathbf{P})$ represents the Jacobian (the determinant of the matrix of derivatives) of the linear transformation defined by \mathbf{P} , from the space of primaries to the gamut in the additive space. The Jacobian in this case will be denoted as $J_{\mathbf{P}}$. The definition in (6) allows on to easily determine the volume when the primaries are scaled, a procedure that is usually performed in white balance process. Let denote by $\gamma = [\gamma_1, \gamma_2, \gamma_3]^T$ the vector with the scale values, then the scaled primaries are obtained as $\mathbf{P}\Gamma\gamma$, where $\Gamma\gamma$ is the diagonal matrix with entries the elements of γ . Using the properties of the determinant, we have that the volume of the gamut for the scaled primaries, $V(\mathcal{G}_{\mathbf{P}\Gamma\gamma}^{XYZ}) = \gamma_1 \gamma_2 \gamma_3 |\det(\mathbf{P})| = \gamma_1 \gamma_2 \gamma_3 V(\mathcal{G}_{\mathbf{P}}^{XYZ})$, that is, the volume is scaled by the product of the scaling factors for the individual primaries.

Using the traditional definition of the gamut in (3), the computation of gamut volume for multiprimary systems is not imme-

diately obvious. The alternative representation introduced in (4) provides an intuitive way for computing the gamut volume. Given that the gamut for a multiprimary system, is composed by the disjoint union of parallelepipeds, which are defined in terms of the gamut enclosed by sets of three primaries, the volume for multiprimary system characterized by the matrix \mathbf{P} , can be expressed as,

$$V(\mathcal{G}^{XYZ}) = \sum_j |\det(\mathbf{P}_j)|, \quad (7)$$

a summation of the gamut volumes $|\det(\mathbf{P}_j)|$, over all possible $\binom{K}{3}$ choices of three primaries from the k columns of \mathbf{P} . This result was previously stated in [9], though without justification.

3.2 Gamut Volume in Perceptual Color Spaces

Perceptually uniform spaces are especially useful to quantify color differences that correlate with observers' assessments. These spaces are obtained by transforming additive spaces by using a nonlinear and space variant function, denoted in this paper by $\mathcal{F}(\cdot)$. Linearity is lost, and therefore definitions of gamut as provided in Section 2 are not feasible. That is, a more accurate representation of color perception is obtained at the expense of losing the benefits of the simplicity of additive spaces. Nonetheless, \mathcal{F} is usually a continuous and differentiable function, which represent an important property to be exploited. For the rest of the document, we base our notation for perceptual spaces on the notation for the standard and widely used CIELAB color space.

The gamut of color perception for a display systems with matrix of primaries \mathbf{P} is obtained by transforming the display gamut from an additive space,

$$\mathcal{G}_{\mathbf{P}}^{LAB} = \left\{ \mathcal{F}(t\mathbf{P}(\alpha)) \mid \alpha \in \mathcal{C}^K \right\}. \quad (8)$$

The parallelepiped that represents the gamut in an additive space is transformed in a non convex solid, as shown in Fig. 2, where the presence of surface concavities can be appreciated. The manipulation of the gamut is difficult, and for the particular case of volume, there is no analytical expression. Approximations for the volume must deal especially with the non-convex shape feature of the solid.

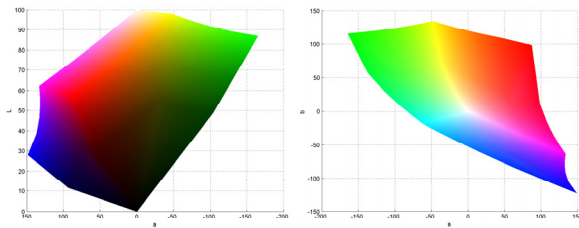


Figure 2. Gamut in CIELAB that is obtained by transforming a gamut in CIEXYZ. In the left a view from the L_a plane, in the right a view from the plane ab

The most general definition for gamut volume is given by,

$$V(\mathcal{G}^{LAB}) = \int \int \int_{[L,a,b] \in \mathcal{G}^{LAB}} dL da db. \quad (9)$$

However, the lacking of an analytical definition for the gamut in perceptual spaces makes difficult the direct computation of the

expression in (9), even by numerical methods. Because \mathcal{F} is non-singular², differentiable and the partial derivatives are continuous, the change of variable theorem can be used to translate the computation of the volume $V(\mathcal{G}^{LAB})$ to a computation of volume over \mathcal{G}^{XYZ} , the gamut in the additive space [10].

For three primary systems, based on the fact that gamut is obtained by a nonsingular linear transformation of the unitary cube, the whole computation can be performed in the space of primaries and the gamut volume can be expressed as follows,

$$V(\mathcal{G}^{LAB}) = \int \int \int_{\alpha \in \mathcal{C}^3} |\mathbf{J}_{\mathbf{P}} \mathbf{J}_{\mathcal{F}}(\mathbf{P}\alpha)| d\alpha_1 d\alpha_2 d\alpha_3, \quad (10)$$

where $\mathbf{J}_{\mathcal{F}}$ represents the Jacobian of the transformation from the additive to the linear space, \mathcal{F} . Note that $\mathbf{J}_{\mathcal{F}}$ must be evaluated at $\mathbf{P}\alpha$.

For multiprimary systems, the decomposition of (4) represents the gamut in CIE XYZ space as a union of disjoint parallelepipeds $\{\mathcal{P}_j\}_j$, where, as indicated earlier, the parallelepiped \mathcal{P}_j is the gamut of the three primary system specified by the primary matrix \mathbf{P}_j displaced by β_j . As a consequence the gamut in CIELAB space can also be obtained as the disjoint union of the transformation of the parallelepipeds, i.e.

$$\mathcal{G}^{LAB} = \bigcup_j \mathcal{F}(\mathcal{P}_j) \quad (11)$$

The nonsingularity of the nonlinear transformation \mathcal{F} , implies that the above expression represents a disjoint union of subgamuts in CIELAB space and the gamut volume in CIELAB can therefore be written as

$$V(\mathcal{G}^{LAB}) = \sum_j V(\mathcal{F}(\mathcal{P}_j)) \quad (12)$$

Each subgamut volume in the summation above can then be obtained in a manner analogous to that used for the three primary system in (10). Specifically, we have

$$V(\mathcal{F}(\mathcal{P}_j)) = \int \int \int_{\alpha \in \mathcal{C}^3} |\mathbf{J}_{\mathbf{P}} \mathbf{J}_{\mathcal{F}}(\mathbf{P}_j\alpha + \beta_j)| d\alpha_1 d\alpha_2 d\alpha_3, \quad (13)$$

Although the expressions in (10), (12), and (13) simplify the expression for volume compared with (9), for the general scenario, an analytical solution does not exist. However, these expressions facilitate the use of numerical methods to obtain accurate results [11], which we develop in the following section.

3.3 Efficient computation of Gamut volume in Perceptual Spaces

In the previous section we translated the computation for gamut volume from perceptual to additive spaces, exploiting their simplicity for gamut representation. In this section we present different methods for the numerical evaluation of the integral in (13). Specifically, we consider a numerical computation of the integral of volume, an estimation based on triangularization of the gamut solid by tetrahedrons, an estimation obtained by computing the convex hull of the gamut and a volume computation based on a local linearization of the perceptual space.

²Strictly speaking, one to one.

As a first step, we note that it can be shown that for the specific case of CIELAB that,

$$J_{\mathcal{F}(X,Y,Z)} = \frac{11600000}{X_w Y_w Z_w} g(X/X_w)g(Y/Y_w)g(Z/Z_w), \quad (14)$$

where,

$$g(t) = \begin{cases} (1/3)t^{-2/3} & \text{for } t > (6/29)^3 \\ (1/3)(29/6)^2 & \text{for } t \leq (6/29)^3 \end{cases}, \quad (15)$$

and $[X_w, Y_w, Z_w]^T$ is a white point reference in CIEXYZ, which, depending on the analysis required, can be selected as the white point of the display.

Based on the fact that \mathcal{F} is a differentiable function, we have by the Taylor's theorem that for every $\mathbf{x}_0 \in \mathcal{G}^{XYZ}$, a point \mathbf{x} satisfy that,

$$\|\mathcal{F}(\mathbf{x}) - \mathcal{F}(\mathbf{x}_0) - \mathbf{J}_{\mathcal{F}}(\mathbf{x}_0)(\mathbf{x} - \mathbf{x}_0)\| \rightarrow 0, \quad (16)$$

as $\mathbf{x} \rightarrow \mathbf{x}_0$ [10]. In equation (16), $\mathbf{J}_{\mathcal{F}}$ is the matrix of partial derivatives of \mathcal{F} , also known as the Jacobian matrix. This means that in small regions around \mathbf{x}_0 the transformation can be linearly approximated³ by the matrix $\mathbf{J}_{\mathcal{F}}(\mathbf{x}_0)$.

Therefore, an approximation for the gamut volume can be obtained by generating a partition of the the gamut in CIEXYZ Space into the union of disjoint and uniform polyhedra of volume v and centered in \mathbf{x}_l , where $l \in L$. A partition in CIEXYZ determines a partition in CIELAB, such that the l -th partition element has a volume v_l^{LAB} , that can be approximated computed as, $v_l^{LAB} = v |J_{\mathcal{F}}(\mathbf{x}_l)|$. In that case the gamut volume can be approximated by

$$V(\mathcal{G}^{LAB}) \approx v \sum_{l \in L} |J_{\mathcal{F}}(\mathbf{x}_l)|. \quad (17)$$

3.3.1 Cubic Tessellation

Different options for the partitioning element and the evaluation point can be done. As a first case, we consider a tessellation made by parallelepipeds. A uniform partition of the gamut (a parallelepiped) is obtained by dividing each of the edges in N equal parts. In that case, all the parallelepipeds share a constant volume given by $J_{\mathbf{P}}/N^3$, and if N is small enough, the linearity assumption is approximately correct, and the gamut volume can be obtained as,

$$V(\mathcal{G}^{LAB}) \approx \frac{J_{\mathbf{P}}}{N^3} \sum_{l \in L} |J_{\mathcal{F}}(\mathbf{x}_l)|. \quad (18)$$

The expression in (18) only requires the computation of the Jacobian for N^3 points, and given the geometry, the center of the parallelepipeds are taken as the evaluation points \mathbf{x}_l

3.3.2 Tetrahedral Tessellation

Every parallelepiped as defined in the previous method is partitioned by six uniform tetrahedra with volume $J_{\mathbf{P}}/(6 * N^3)$. In this way, we obtain a finer set of sample points, and their distribution

³A local linearization of CIELAB has previously been effectively utilized in defining analytically computable metrics for color recording devices that correlate well with perceptual color errors [12].

in the space makes possible to capture some more information that a cubic interpolation does not provide. A similar expression as in (18) can easily be inferred. A natural point for the Jacobian evaluation is the *centroid* of every tetrahedron. However, different tessellations of a parallelepiped can be obtained, leading to different sample points. As shown in Section 4, that different selections lead to very different performance, specially when the gamut subdivisions are small in number.

One of the possible tetrahedral partitions of a cube is obtained by imposing the constraint that the main diagonal of the cube belongs to every tetrahedron. This practice is commonly used in other applications like interpolation for color space conversions, where the "device gray" axis plays a significant role [13]. The gray region still plays an important role in the context of volume computation, due to its perceptual significance that can be expressed in terms of volume. However, applying the strategy of partitioning along a shared main diagonal is disadvantageous. The gray axis constraint determines tetrahedrons that cover very similar regions around the gray label, and therefore the centroids are located far from this region, losing important information in perceptual changes and leading to poorer approximations. On the other hand, a partition where every tetrahedron covers different regions of the gray axis, is able to distribute centroids that better capture perceptual changes, providing a more accurate approximation. The results in Section 4 validate this analysis.

An adequate selection of a partition highlights the importance of selecting the sample points, in this case determine by the centroids of the tetrahedrons. The centroid is a natural point to choose, and it is easy to compute. Nevertheless, there are other points that characterize a tetrahedron, being one of them the *incenter*. As described in next section, the incenter points offer better approximations, although its computation is more involved.

Finally, it is important to mention that in a more general scenario, the volume of each partition element can be approximated by sampling in more than one point inside the volume, that is, $v_l^{LAB} = v \sum_i^m w_i |J_{\mathcal{F}}(\mathbf{x}_{i,l})|$, where $\{w_i\}_{i <= m}$ represent weight factors, not necessary positive, for sample points $\{\mathbf{x}_{i,l}\}$, and satisfy $\sum_i w_i = 1$. General rules for choosing the number and the location of the sample points have been developed in the context of finite element analysis [14, 15]. A particular selection is taken based on a trade-off between efficiency and accuracy.

3.3.3 A Nonlinear Approximation by Tetrahedral Elements

The linear approximation developed suggest also that the polyhedrons that tessellate the gamut in the linear space, are approximately transformed into polyhedrons in a perceptual space. In that sense, once the tessellation is obtained in the linear space, by following the same strategy as in Section 3.3.2, the vertexes of the tetrahedrons are transformed to the perceptual space, by means of the non linear transformation \mathcal{F} , and assuming that they are still vertexes of tetrahedrons, the volume for all the solids are computed and summed up.

4 Results

The different methodologies described in Section 3.3 were evaluated for three primary and multiprimary systems. For the three primary case, we compute the gamut volume for the configurations of primaries shown in Table 2. They include a set of

primaries that match chromaticity values of important standards, and arbitrary configurations selected by the authors. The volumes in CIELAB space obtained from the numerical integrations are also included.

As a first step, we evaluated the performance between different choices for tetrahedral partitioning. Figure 3 shows two possible tetrahedral tessellations of a cube and their effect on the distribution of the centroids. The partition which tetrahedrons share the gray axis distributes the centroids (labeled as circles) far from the white and dark regions. In the other partition the gray axis does not belong to any tetrahedron, but crosses all of them. In the latter case, the centroids are distributed along the gray axis. In fact for this case, every tetrahedron covers a different region along of the gray direction, better representing the change in perceptual space. The difference in the performance between these two configurations when estimated the volume for the configuration C5 in Table 1, can be appreciated in the bottom of Fig. 3, where the second case offers a more accurate estimation for the same number of subdivisions comparing to the traditional partitioning, and converging the computation to the result faster. If instead, the volume estimation is based on the incenters, the accuracy is even greater, and the convergence faster. For the next comparisons, and whenever we refer to the *tetrahedra tessellation method*, we will estimate the gamut volume on the incenters of the the second partition described.

		C.1	C.2	C.3	C.4	C.5
P_1	x	0.64	0.68	0.64	0.4605	0.7273
	y	0.33	0.32	0.33	0.2105	0.0909
P_2	x	0.30	0.265	0.21	0.1429	0.1429
	y	0.60	0.69	0.71	0.5714	0.6429
P_3	x	0.15	0.15	0.15	0.1875	0.1250
	y	0.06	0.06	0.06	0.1875	0.2500
Y_W		100	100	100	1.4	1.4
$V(\mathcal{G}^{LAB})$		0.8873	1.3399	1.2298	0.3865	0.8727

Table 2. Chromaticity coordinates and luminance of the white point for the set of primaries tested. The configurations C_1, C_2, C_3 correspond to chromaticity values for REC 709 [16], RP 431-2 [17], and ADOBE RGB [18], respectively. The other two configuration were selected arbitrary by the authors. The perceptual volume $V(\mathcal{G}^{LAB})$ for each configuration is also shown in $\Delta E_{L,A,B}^3 \times 10^6$ units.

As the next step we compare the performance between the other numerical methods proposed. The results of evaluating the linear approximations by cubic tessellation, tetrahedral tessellation, the tetrahedral approximation using four sample points⁴ and the nonlinear approximation by transforming the tetrahedral tessellation, are shown in Fig. 4, that shows the convergence of gamut volume computation for the tested configurations as a function of the number of partitions along the edges of the gamut in the linear color space. For few partitions, the cubic approximation presents very poor estimations, when clearly the assumption of linearity is not completely valid. The tessellation based on tetrahedral elements provides better estimates, as a result of more sample points (for every cube there are six tetrahedra) and better

⁴The weights and locations of the points are chosen according to [14].

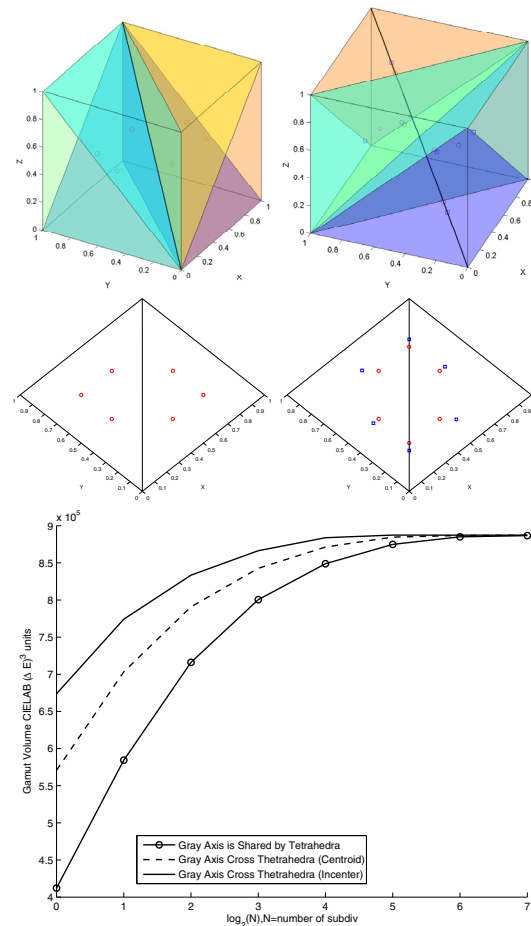


Figure 3. In the top, two tetrahedra partitions of the cube. In the middle, the distribution of the centroids (circles) for both configurations, compared to gray level axis (line between (0,0,0) and (1,1,1)). In the left, the gray axis belongs to all tetrahedrons and distributes centroids far from gray region. In the right, the gray axis does not belong to any tetrahedron, but cross all of them, distributing centroids along the gray axis. The incenters in the later case (square) are located toward the boundary of the cube. The bottom shows the gamut volume computation in terms of the number of divisions for the three cases described: one sharing the gray axis, one where gray axis crosses the tetrahedra and the volume is evaluated in the centroid, one where gray axis crosses the tetrahedrons and the volume is evaluated in the incenter.)

		C.1	C.2	C.3
P_1	X	0.6700	0.6400	0.6392
	Y	0.3250	0.3300	0.3299
P_2	x	0.2841	0.3008	0.3008
	y	0.6829	0.5989	0.5989
P_3	X	0.0869	0.1501	0.1499
	Y	0.5710	0.0600	0.0599
P_4	x	0.1399	0.4905	0.3130
	y	0.0450	0.5000	0.3282
Y_W		0.8798	497	602
$V(g^{LAB})$		1.6030	0.7293	0.5351

Table 3. CIEXYZ coordinates for a set of four primaries systems. The M_1 system is proposed in [7] and defined in (5), while M_2, M_3 were arbitrarily selected by the authors. The perceptual volume $V(g^{LAB})$ for each configuration is also shown in $\Delta E_{L,A,B}^3 \times 10^6$ units.

distribution of these points in the space. In particular, it can be appreciated that the estimation is better by using four points per tetrahedron. The use of more points have a cost in computation. In Fig. 5, where the mean computational time required to complete the volume computation is shown as a function of the partitions. Clearly the cubic tessellation offers the lowest cost compared to the other methods. The cost in computation increases for the linear approximation by tetrahedral elements as long as the number of partitions increases, specially when the number of points per tetrahedron to evaluate increases.

Finally the estimation obtained by transforming a tetrahedral tessellation and computing the volume presents very good estimations. The accuracy is better than the obtained by the cubic approximation, and it is very similar compared to the other tetrahedral methods. However, the computational cost is considerably higher, specially for lower number of partitions. The cost is mainly due to the transformation from linear to the perceptual space.

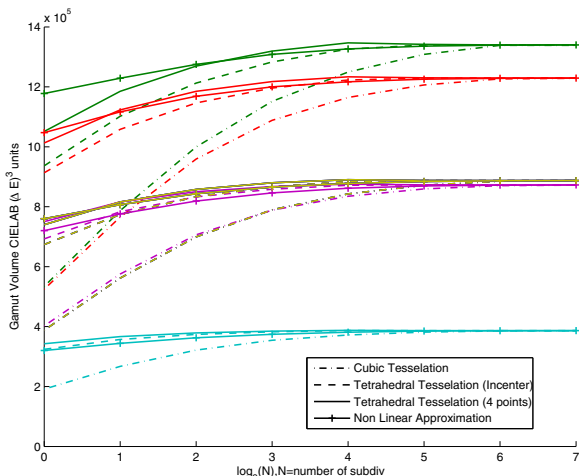


Figure 4. Convergence of gamut volume computation, for the systems defined in Table 2, in terms of the number of divisions.

Based on the methodology outlined in (12)–(13), the algorithm were applied to compute volume for the multi-primary configurations defined in Table 3 Figure 6 shows a plot of the es-

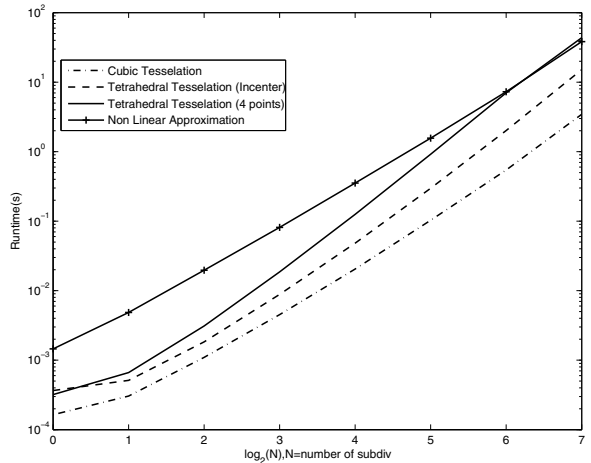


Figure 5. Computational time as a function of the number of divisions. All computations were performed in a Matlab environment on a desktop, having a AMD Athlon 64 X2 2.0 GHz CPU with 1.9 GB memory.

timated gamut volume obtained with the different methods as a function of the number of subdivisions along each of the parallelepiped axes. The results mirror the trends seen for the three primary case in Fig. 4. With adequate number of subdivisions, the local linearization methods offer an accurate estimate of the gamut volume at a low computational cost. However, in this case, the nonlinear transformation seems to offer the most accurate results. Although the linear approximations, specially those based on tetrahedral tessellation, offer very good approximations, it is evident the performance is poorer. One possible reason for this anomalous behavior is based on the gamut representation. In a similar way as the choice of tetrahedral partition for the cube influences the results, different gamut representations offer different coverage of perceptually important regions and thus, different performance in volume gamut estimation. A study of the effect on the selection of gamut representation is still pending.

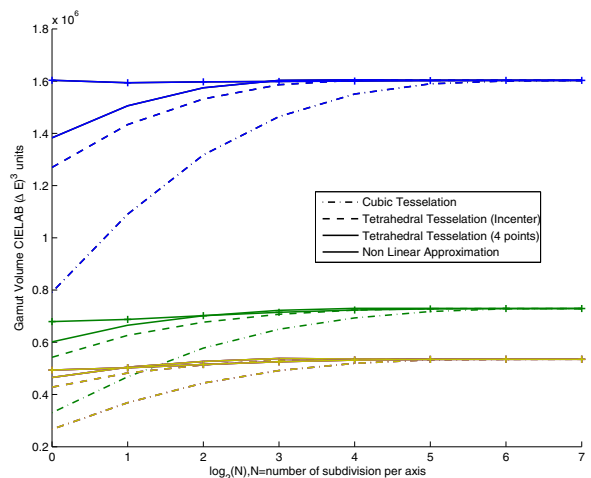


Figure 6. Volume estimation using the numerical methods proposed, for the multi-primary systems defined in Table 3, as a function of the number of divisions of the parallelepiped axes.

5 Conclusion

We presented a methodology for computing gamut volumes for three primary and multi-primary displays in perceptual spaces that exploits gamut representations in additive color spaces to develop computationally efficient numerical schemes for evaluating gamut volume. Specifically, for multi-primary displays, we develop an alternative gamut representation that simplifies gamut volume computation. Four numerical schemes were compared with respect to accuracy and cost for the purpose of computing gamut volumes in the proposed framework. Our results demonstrate that the proposed framework offers accurate results when adequate number of subdivisions/sampling points are employed. Among the alternatives explored, a cubic tessellation with an optimized subdivision of the cubes into tetrahedra, offered the most accurate results for a given computational load.

Modifications to the overall algorithm to obtain more efficient results are still possible and constitute ongoing work. Specifically, the current work has explored equal number of subdivisions along the different parallelepiped axes and equi-spaced subdivisions along each axes. Simple modifications allow for unequal subdivisions with minimal increase in computational cost, these will be explored in our continuing work.

References

- [1] W. N. Sproson, *Colour science in television and display systems*. Bristol: Adam Hilger Ltd, 1983.
- [2] R. W. G. Hunt, *The Reproduction of Colour*, 6th ed. West Sussex, England: John Wiley and Sons Ltd., 2004.
- [3] CIE, "Colorimetry," CIE Publication No. 15.2, Central Bureau of the CIE, Vienna, 1986, the commonly used data on color matching functions is available at the CIE web site at <http://www.cie.co.at/>.
- [4] G. Sharma and H. J. Trussell, "Digital color imaging," *IEEE Trans. Image Proc.*, vol. 6, no. 7, pp. 901–932, Jul. 1997. [Online]. Available: <http://www.ece.rochester.edu/~gsharma/papers/dciip97.pdf>
- [5] G. Sharma, "Color fundamentals for digital imaging," in *Digital Color Imaging Handbook*, G. Sharma, Ed. Boca Raton, FL: CRC Press, 2003, chapter 1.
- [6] —, "LCDs versus CRTs: Color-calibration and gamut considerations," *Proc. IEEE*, vol. 90, no. 4, pp. 605–622, Apr. 2002, special issue on Flat Panel Display Technologies.
- [7] S. Wen, "Design of relative primary luminances for four-primary displays," *Displays*, vol. 26, no. 4-5, pp. 171 – 176, 2005. [Online]. Available: <http://www.sciencedirect.com/science/article/B6V01-4GR32TK-3/2/f1f48d1d27bb992f0eb0ca05e5c5f438>
- [8] C. Meyer, *Matrix analysis and applied linear algebra*. Philadelphia, PA: Society for Industrial and Applied Mathematics, 2000.
- [9] G. Sharma, "Set theoretic estimation for problems in subtractive color," *Color Res. Appl.*, vol. 25, no. 4, pp. 333–348, October 2000. [Online]. Available: <http://www.ece.rochester.edu/~gsharma/papers/subcolpocsCRNA2000.pdf>
- [10] J. Marsden and A. Tromba, *Vector Calculus*. New York, NY: W.H. Freeman and Company, 1988.
- [11] R. Burden and J. D. Faires, *Numerical Analysis*. Boston, MA: Brooks/Cole Cenegage Learning, 2005.
- [12] G. Sharma and H. J. Trussell, "Figures of merit for color scanners," *IEEE Trans. Image Proc.*, vol. 6, no. 7, pp. 990–1001, Jul. 1997. [Online]. Available: <http://www.ece.rochester.edu/~gsharma/papers/fomip97.pdf>
- [13] J. M. Kasson, S. I. Nin, W. Plouffe, and J. L. Hafner, "Performing color space conversions with three-dimensional linear interpolation," *J. Electronic Imaging*, vol. 4, no. 3, pp. 226–250, Jul. 1995.
- [14] M. Gellert and R. Harbord, "Moderate degree cubature formulas for 3-d tetrahedral finite-element approximations," *Communications in Applied Numerical Methods*, vol. 7, no. 6, pp. 487–495, 1991.
- [15] G. Bedrosian, "Shape functions and integration formulas for three-dimensional finite element analysis," *International Journal for Numerical Methods in Engineering*, vol. 35, no. 1, pp. 95–108, 1992.
- [16] *REC. ITU-R BT.709 HDTV: Parameter values for the HDTV standards for production and international programme exchange*. International Telecommunication Union, accessed April 2011. [Online]. Available: <http://www.itu.int/>
- [17] *Color Processing for D-Cinema*. Society of Motion Picture and Television Engineers, accessed April 2011. [Online]. Available: <http://www.smpte.org>
- [18] *Adobe RGB(1998) Color Image Encoding*. Adobe Systems Incorporated, accessed April 2011. [Online]. Available: <http://www.adobe.com/>